# Generation of core-shell microcapsules with three-dimensional focusing device for efficient formation of cell spheroid†

Choong Kim,[a] Seok Chung,[b] Young Eun Kim,[a] Kang Sun Lee,[c] Soo Hyun Lee,[a] Kwang Wook Oh[c] and Ji Yoon Kang*[a]

*Received 18th May 2010, Accepted 9th September 2010*
**DOI: 10.1039/c0lc00036a**



We present a microfluidic device generating three-dimensional (3D) coaxial flow by the addition of a simple hillock to produce an alginate core-shell microcapsule for the efficient formation of a cell spheroid. A hillock tapered at downstream of the two-dimensional focusing channel enables outside flow to enclose the core flow. The aqueous solution in the core flow was focused and surrounded by 1.8% alginate solution to be solidified as a shell. The double-layered coaxial flow (aqueous phase) was broken up into a droplet by the shear flow of oleic acid (oil phase) containing calcium chloride for the polymerization of the alginate shell. The droplet generated from the laminar coaxial flow maintained a double-layer structure and gelation of the alginate solution made a core-shell microcapsule. The shell-thickness of the microcapsule was adjusted from 8–21 μm by the variation of two aqueous flow rates. The inner shape of the shell was almost spherical when the ratio of the water–glycol mixture in the core flow exceeded 20%. The microcapsule was used to form a spheroid of embryonic carcinoma cells (embryoid body; EB) by injecting a cell suspension into the core flow. The cells inside the microcapsule aggregated into an EB within 2 days and the EB formation rate was more than 80% with strong compaction. The microcapsule formed single spherical EBs without small satellite clusters or a bumpy shape as observed in solid microbeads. The microfluidic chip for encapsulation of cells could generate a number of EBs with high rate of EB formation when compared with the conventional hanging drop method. The core-shell microcapsule generated by 3D focusing in the microchannel was effective in forming large number of spherical cell clusters and the encapsulation of cells in the microcapsule is expected to be useful in the transplantation of islet cells or cancer stem cell enrichment.

## 1. Introduction

Cell microencapsulation is an appropriate method of forming spherical cell bodies, and is an important component of tissue engineering applications like organ bioprinting or cell therapy applications.[1–5] A variety of materials including poly(lactic-*co*-glycolic acid) (PLGA), collagen, hyaluronic acid (HA), polyethylene glycol (PEG), gelatin, agarose and alginate have been used for the encapsulation of cells, and are chemically modified for their own purposes. For example, the alginate-PLL (poly-L-lysine)-alginate (APA) membrane of the alginate capsule controls the molecular cutoff value. It passes nutrients, proteins, DNA and anticancer drugs, but blocks antibodies and immune cells for the immunoisolation of pancreatic islets.[6–8] The various functions of microcapsules have brought new initiatives to many applications for pharmaceutics, food and cosmetics.[9–11]

Microcapsules from bulk emulsifications are capable of containing a variety of contents;[12–21] however, these methods have difficulties in live cell encapsulation due to the damage to cells in the complex processes of surface functionalization, particle coating, subsequent chemical reaction, washing, centrifugation and redispersion. Recently, microfluidic techniques have achieved much progress in cell encapsulation with alginate using a two-phase micro-emulsion technique. This approach preserves cell viability as well as mono-dispersity of microcapsules.[22,23] Internal gelation of alginate using $CaCO_3$ nanoparticles in microfluidic channels enhances the viability of human leukemic cells (Jurkat) by flushing out hydrochloric acid solution with buffer.[22] In another study, the exchange of toxic oleic acid-containing calcium chloride with harmless mineral oil also improved the viability of several cell lines including P19 EC, MCF 7 and HepG2.[23] Solid alginate microbeads are useful in encapsulated cell culture, but are ineffective in forming a spheroid cell body. The hydrogel between cells interrupts direct cell-to-cell interaction and several clusters of cells are generated in a microbead with the low rate of single spheroidal cell body formation (<10%). A hollow core-shell microcapsule is more adequate for aggregating cells in microcapsule than solid microbeads.

APA microcapsule consists of hollow microcapsules with a liquefied alginate core. The surface of the alginate microbead is linked to PLL and alginate sequentially with charge interaction, and then the alginate core is liquefied by tri-sodium citrate (TC) treatment.[24,25] APA is effective in aggregating cells to form a spheroid; however, the membrane is mechanically weak and alginate can affect the encapsulated cells in assay results (*e.g.*,

[a]*Nano-Bio Research Center, Korea Institute of Science and Technology, 136-791 Seoul, Korea. E-mail: jykang@kist.re.kr; Tel: (+82)-2-958-6747*
[b]*School of Mechanical Engineering, Korea University, Korea*
[c]*Department of Electrical Engineering, University at Buffalo, The State University of New York, USA*

† Electronic supplementary information (ESI) available: Cell viability test of P 19 EC cells; supplementary movies 1–3. See DOI: 10.1039/c0lc00036a

 

differentiation of stem cells). Liquefying with TC can damage the encapsulated cells, especially when the diameter of the capsule is <200 μm. *In situ* synthesis methods like a thermo-sensitive or ultraviolet (UV) -sensitive polymer shell are utilized for hollow microcapsules, but require a high temperature (>60 °C) or UV light, which can induce apoptosis of living cells by heat-shock or UV irradiation.[26–29] Without a harmful polymerization process or complicated post-processing, a multi-layered glass capillary for three-dimensional (3D) coaxial flow could generate hollow microcapsule containing cells; however, controlling the diameter of glass capillaries is onerous and assembling multi-layered glass capillaries requires delicate handling.[30,31]

This paper presents a new method producing 3D coaxial flow by means of a hillock structure in a microfluidic focusing channel. We encapsulated P19 mouse embryonic carcinoma cells in core-shell microcapsules and demonstrated the effective formation of uniform massive embryoid bodies (EB) for the study of stem cell differentiation.

## 2. Experimental

### 2.1 Microfabrication

The microfluidic device was fabricated by a multi-level SU-8 fabrication method[32] and replica molding. SU-8 2025 (Microchem, Newton, MA) and SU-8 2050 (Microchem) were used for the 2-layered SU-8 microstructures. In brief, the first layer, which had a height of 25 μm, was patterned on a silicon wafer by spinning a SU-8 photoresist (SU-8 2025) and exposure of the first layer with a photomask. After post-bake, a second layer of photoresist, which was 75 μm high, was formed with SU-8 2050. Both SU-8 layers were subsequently developed simultaneously. Next, polydimethylsiloxane (PDMS, Sylgard 184; Dow Corning, Midland, MI) was poured onto master molds for top and bottom slabs. After curing, the PDMS replicas were peeled off from the two master molds. Holes were then punched through the PDMS slab to prepare inlets and outlets.

After air plasma treatment, the two PDMS slabs with hillock geometry were aligned and bonded.[33] In brief, the two PDMS slabs treated by air plasma were dipped into a high-purity methanol (99.9%) to prevent instant bonding and to allow smooth movement between each layer during stacking and alignment. The precise alignment of both layers was controlled by hand under a stereo zoom microscope (Olympus SZ 51, Tokyo, Japan). Once the alignment was completed, the pre-bonded PDMS slabs were placed on a hot plate for 80 min at 85 C to evaporate methanol between the two layers. The tolerances on the top-bottom alignments were less than ±5 μm. In that tolerance range, there was no problem on the generation of core-shell microcapsules in the experiments.

Since the surface property of the PDMS device was altered from hydrophobicity to hydrophilicity after the plasma treatment, the device was utilized after 2 days for the recovery of hydrophobicity.

### 2.2 Image analysis

The formation of droplets and the encapsulation of cells were observed using a FASTCAM-Ultima 512 Imager high-speed CCD video camera (Photron, Tokyo, Japan) installed on a IX2-SLP phase inverted microscope (Olympus, Tokyo, Japan), where the images were recorded at 2000 frames/s. Cross-sections of the microcapsule were photographed by confocal microscopy (Axicam, Zeiss, Germany) to visualize the 3D core-shell structure of microcapsules. Alginate in microcapsules or microbeads was stained with Alexa fluor. The carboxylic acid groups of alginate were activated with a mixture of 10 mg of *N*-(3-dimethylaminopropyl)-*N*′-ethylcarbodiimide hydrochloride (EDC, Sigma-Aldrich, St. Louis, MO). Goat anti-mouse antibody with Alexa fluor 555 was linked to the activated region in 1 mL of deionized water overnight at 4 °C.

### 2.3 Materials

Sodium alginate (A2158-250G, Sigma-Aldrich) was dissolved in culture medium (α-MEM, Gibco, Grand Island, NY) to a final concentration of 3.6% (w/v) and the solution was filtered using a 0.2 μm syringe filter (PALL Life Science, Port Washington, NY) to remove bacteria and any clumps of alginate. P19 mouse embryonic carcinoma (mEC) cells were released from the culture dish surface by 0.25% Trypsin EDTA (Gibco), and were centrifuged for 5 min at 600 rpm. The cell suspension was mixed with 1.8% alginate in α-MEM. Oleic acid was utilized as a continuous phase to generate alginate droplets. Alginate was gelified by infused calcium in oleic acid. Calcium chloride (2.1 g) (C7902-500G; Sigma-Aldrich) was dissolved in 50 mL of 2-methyl-1-propanol (Junsei Chemical< Tokyo, Japan) in a model 5510 ultrasonication bath (Branson, Danbury, CT). After mixing the calcium solution and oleic acid at a ratio of 50% (v/v), the 2-methyl-1-propanol was distilled overnight on a model HHP-401 hotplate (Shamal, Tokyo, Japan) at 120 °C. Finally, the oleic acid with calcium was filtered with a syringe filter (0.2 μm) to remove any debris. The calcium in oleic acid polymerized the alginate solution in the microchannel.

### 2.4 Cell culture and cell viability assays

The mEC cell line, P19 EC, was acquired from American Type Culture Collection (CRL1825; Manassas, VA). P19 EC cells were cultured in α-MEM (Gibco) supplemented with 10% fetal bovine serum (FBS), 1% penicillin and streptomycin (all from Gibco). P19 EC cells were maintained at 37 °C in a humidified atmosphere of 5% $CO_2$ and passaged at 2 or 3 day intervals. Trypan blue staining was used to identify living and dead cells. All toxicity assays were repeated three times.

## 3. Results and discussion

### 3.1 Principle of 3 dimensional coaxial flows in microchannel

The microfluidic device for 3D coaxial flow is comprised of two PDMS slabs with hillock-embedded microchannels (Fig. 1(a)). The device has three parts for the encapsulation of cells in a core-shell alginate capsule: a 3D focusing part for core-shell flow generation, a droplet generation part for the encapsulation of cells and a fluid exchange part for the maintenance of cell viability. They are positioned from upstream to downstream sequentially. Top and bottom microchannels with a depth of 100 μm each are aligned and bonded, and the height of each hillock is

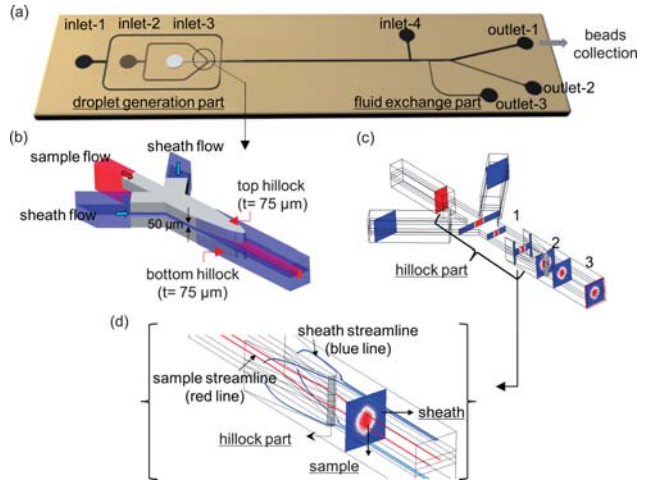


**Fig. 1** Principle of 3D coaxial flows in microchannel for the generation of core-shell microcapsules. (a) The microfluidic device for 3D coaxial flow comprised two PDMS slabs with hillock-embedded microchannels. The device has three parts: a 3D focusing part for core-shell flow generation, a droplet generation part for the encapsulation of cells and a fluid exchange part for the maintenance of cell viability. (b) The height of each hillock was 75 μm. The depth of microchannel was 200 μm except the hillock region with the gap of 50 μm. (c) The procedures of 3D hydrodynamic focusing in microchannel. The core flow was squeezed in two-dimensions by two sheath flows in shallow hillock region (1) and then the focused flows enter the tapered region of hillock, sheath flows occupy the upper and lower part of the core flow and at the end of hillock they circumvent the core flow (2 and 3). (d) The stream of core flow cannot reach the top and bottom wall of microchannel due to the preoccupation of the sheath flows.

75 μm. The depth of the microchannel is 200 μm, except for the hillock region with the gap of 50 μm (Fig. 1(b)).

The core flow was squeezed in two dimensions by two sheath flows in the shallow hillock region (Fig. 1(c)-1). When the focused flows enter the tapered region of hillock, the outside portion of the sheath stream near the wall of the side channel expands to the top and bottom wall where the cross-section of the microchannel looks like a bobbin or I-beam. Then, the expanded sheath flows occupy the upper and lower parts of the core flow and at the end of hillock they circumvent the core flow (Fig. 1(c)-2, and 1(c)-3). The stream of core flow cannot reach the top and bottom wall of microchannel due to the earlier stream of the sheath flows (Fig. 1(d)). As a result, the hillock structure induces a centered core flow that is completely surrounded by an outer sheath flow with facile flow control (supplementary movie 1† (CFD RC, ESI-CFD, USA)).

### 3.2 Generation of core-shell microcapsules and solid microbeads

To generate core-shell microcapsules, oleic acid containing calcium chloride, sodium alginate solution and a 80% water-glycerol mixture (using sodium alginate solution for the generation of solid microbeads) were injected respectively from inlet 1 (350 μL $h^{-1}$), inlet 2 (50 μL $h^{-1}$) and inlet 3 (100 μL $h^{-1}$) *via* syringe pumps (KD Scientific, Holliston, MA) (Fig. 2(a) and

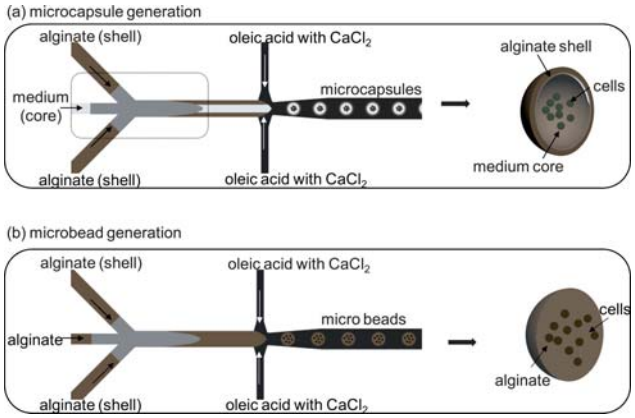


**Fig. 2** The generation of core-shell microcapsule and solid microbead. (a) In order to generate core-shell microcapsule, oleic acid, sodium alginate solution and 80% glycerol were injected respectively from inlet 1 (350 μL $h^{-1}$), inlet 2 (50 μL $h^{-1}$), and inlet 3 (100 μL $h^{-1}$) *via* syringe pumps. (b) When we substituted the water-glycol with sodium alginate solution, solid alginate microbeads were also generated the generation of solid microbeads.

2(b)). Downstream, mineral oil was injected from inlet 4 (7.5 mL $h^{-1}$) to remove the toxic oleic acid (Fig. 1(a)).[23]

The water-glycerol (80% v/v) mixture was hydrodynamically focused three-dimensionally by two lateral alginate solutions (1.8%). The water-glycol solution surrounded by the alginate flow was broken up into droplets by oleic acid, and infiltrated calcium chloride in oleic acid gelified the alginate shell downstream of the microchannel and finally formed core-shell microcapsules (Fig. 2(a), supplementary movie 2†). When we substituted the water-glycol with sodium alginate solution, solid alginate microbeads were also generated (Fig. 2(b)).

Confocal microscopy images confirmed the difference of core-shell microcapsules and microbeads, where the alginate was stained with Alexa fluor. Fig. 3(a) and 3(b) depict the cross-sections of a microcapsule and a microbead, respectively, sliced in the *z*-axis from the top to bottom, and also the fluorescent intensity profile of section d. The diameter of a microcapsule was 130 μm with a shell thickness was about 8 μm.

### 3.3 The effect of flow rate and viscosity of core on the shell structure

The shell thickness of a microcapsule is adjusted by the ratio of the core flow and the sheath flows. Sectional views of the microcapsules are shown in Fig. 4(a) produced with different flow ratios of 1 : 4 : 1, 1 : 2 : 1, and 1 : 1 : 1 (shell : core : shell = alginate : 80% water-glycerol mixture : alginate = 25 : 100 : 25, 37.5 : 75 : 37.5, 50 : 50 : 50 μL $h^{-1}$). The thickness of shells increased with the increment of the ratio of core flow rate and the sheath flow (8 μm, 14 μm, and 21 μm).

A core solution with higher viscosity generated a more stable capsule shape with a thinner shell (Fig. 4(b)). We adjusted the viscosity of the core flow with the addition of the glycerol to water. Undulatory or irregular shapes of shell cross-section were observed when the core was less viscous. This was attributed to the abrupt blocking of core flow caused by "pinch-offs" or break-up in droplet generation. While large viscosity prevents the

 

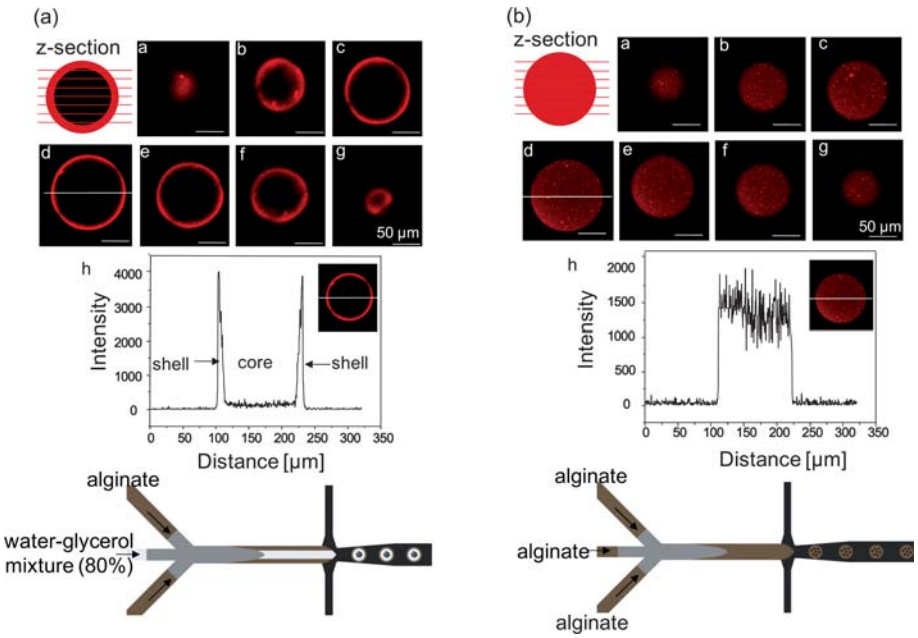


**Fig. 3** *z*-Axial sectioning images of microcapsule by confocal microscopy. Confocal microscopy images confirmed the shape of the generated microcapsules and microbeads. With a view of visualization the state of the interior, core-shell microcapsules and solid microbeads were stained with Alexa fluor dyes *via* EDC-mediated crosslinking, which stained only alginate. (a) Cross-sections of a microcapsule sliced in the *z*-axis from top to bottom and also the fluorescent intensity profile of section d. The diameter of a microcapsule was 130 μm with a shell thickness of about 8 μm. (b) This figure indicates *z*-axis sectional view regarding the gelified solid microbead and the interior of microbead is filled and solidified by alginate.

turbulent flow by shear friction, the core flow with low viscosity cause oscillations or fluctuations in microcapsule since the inertia of moving fluid dominates the shear friction.[34] Additionally, the thickness of the microcapsule shell appeared to increase under identical flow rate conditions, because the alginate solution (1.8%) and glycerol-water mixtures (<80%) were mixed by turbulent flow prior to gelation in the downstream channel.

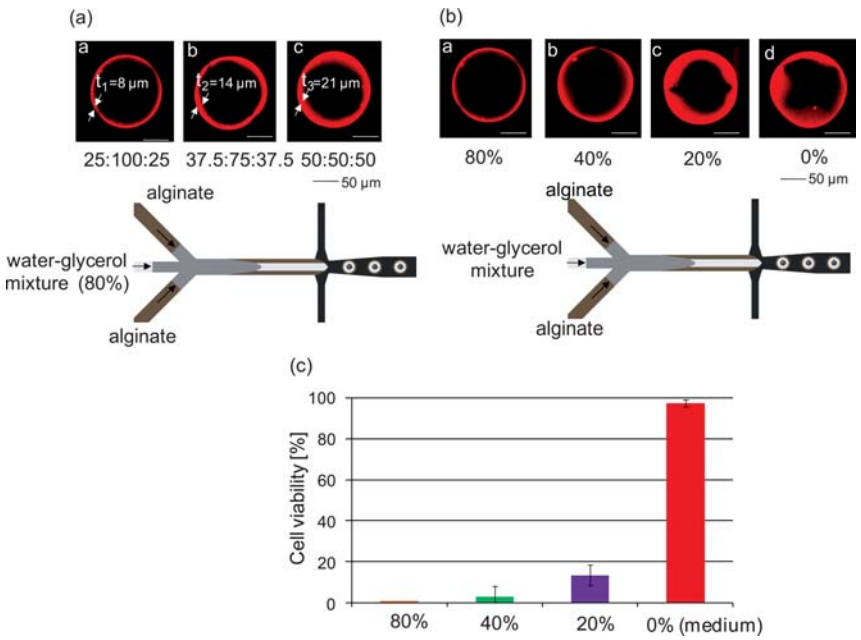


**Fig. 4** Control of shell thickness, the effect of viscosity of core solution, and cell viability on the water-glycerol mixtures. (a) The shell thickness of microcapsule is adjusted by the ratio of the core flow and the sheath flows (shell : core : shell = 1 : 4 : 1, 1 : 2 : 1, and 1 : 1 : 1). The thickness of shells increased with the increment of the ratio of core flow rate and the sheath flow (a: 8 μm, b: 14 μm, and c: 21 μm). (b) A core solution with higher viscosity generated more stable capsule shape with a thinner shell (Fig. 4(b)-a). Undulatory or irregular shapes of shell cross-section were observed when the core was less viscous (Fig. 4(b)-b–d). (c) The viability of P19 EC cells was tested to investigate the toxicity of glycerol with the mixtures of glycerol and culture medium (80%, 40%, 20%, and 0%). The cell viability increased with the decrement of glycerol concentration; 0.3% (SD = 0.1), 2.97% (SD = 5.15), 13.5% (SD = 4.95), and 97.4% (SD = 1.76).

The viability of P19 EC cells was tested to investigate the toxicity of glycerol with the mixtures of glycerol and culture medium (80%, 40%, 20%, and 0%) (Fig. 4(c)). P19 EC cells were added to a tube containing glycerol-medium mixtures and then were placed in an incubator at 37 °C for 10 min. The cell viability increased with the decrement of glycerol concentration; 0.3% (SD = 0.1), 2.97% (SD = 5.15), 13.5% (SD = 4.95), and 97.4% (SD = 1.76). Due to the toxicity of glycerol to P19 EC cells, medium with low viscosity was utilized as a core despite of the irregular shape of core, to improve cell aggregation in microcapsule.

### 3.4 Generation of triple-layered microcapsule

Addition of a 3D focusing region enabled a microfluidic device to generate triple-layered microcapsules (supplementary movie 3†). Theoretically, the number of focusing regions determines the number of microcapsule layers. Triple-layered microcapsules were produced by double 3D focusing (Fig. 5(a)). The first layer was culture medium with red microbeads, the second layer was sodium alginate without fluorescence tag, and the last layer was sodium alginate with green microbeads. Fluorescent microbeads were mixed with solution for the visualization of triple-layered microcapsules. Culture medium with red fluorescent microbeads of 10 μm diameter (Duke Scientific, Fremont, CA) was focused by alginate solution. The previously focused streams were focused again by the additional alginate solution flow with green fluorescent microbeads of 1 μm diameter (Duke Scientific).

The cross sectional shape of core flow is determined by the geometry of focusing channel and the ratio of core flow to sheath flow. For the circular core flow, we adjusted the ratio of flow and the taper angle to 1 and less than 60°, respectively. The eccentricity of elliptical cross section is readily controlled by the adjustment of flow ratio. The flow rate of each sodium alginate solution was 50 μL $h^{-1}$ and that of oleic acid was 350 μL $h^{-1}$. The cross-sectional fluorescent image and intensity profile of a triple-layered microcapsule were acquired by confocal microscopy (Fig. 5(b) and 5(c)). The absence of mixing of the fluorescence colors between layers confirmed that the three layers of microcapsule were successfully formed. The second or third layer can be used to affect the cells in core (the first layer). For example, stem cells in the core can be co-cultured with terminally differentiated cells in the surrounding shell for directed differentiation. The alginate layers can contain functional micro or nanobeads or drug for further applications such as fluorescence tagging, magnetic manipulation or sequential drug delivery.

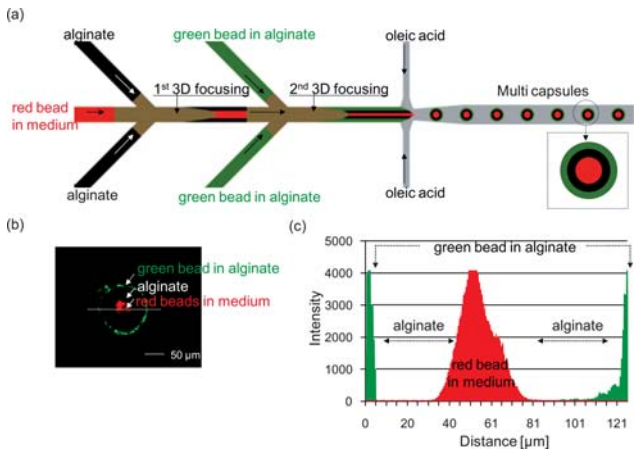


**Fig. 5** Triple microcapsule generation. (a) Triple-layered microcapsules were produced by double 3D focusing. The first layer was culture medium with red microbeads, the second layer was sodium alginate without fluorescence tag and the last layer was sodium alginate with green microbeads. The previously focused streams are focused again by the additional alginate solution flow with green fluorescent microbeads of 1 μm diameter. (b) and (c) The cross-sectional fluorescent image (b) and intensity profile (c) of a triple-layered microcapsule were acquired by confocal microscope.

### 3.5 Efficient formation of massive EBs

The cell suspension of culture medium without glycerol was injected in the core and the alginate solution was flowed into outside flows to induce the spheroid formation of some mammalian cells. Several kinds of cells like hepatocyte or stem cells tend to aggregate and form a spheroid effectively inside alginate microcapsule because the surface of sodium alginate prevents the adhesion of cells.[35] The cells in 1.8% alginate solution have almost same viability as those in culture medium (Fig. S-1, ESI†). The encapsulated cells in microcapsule or microbead also demonstrated no less viability than those before encapsulation process.

We compared the efficiency of spherical EB formation with P19 EC cells. EC cells were cultured for 2 days in core-shell microcapsules and also in solid microbeads (Fig. 6(a)). More than 90% of the cells were alive in both microcapsule and microbeads (Fig. 6(b)). The cells in the microcapsules aggregated more easily than those in the solid bead. Liquid core in the microcapsule was effective in single EB formation without satellite EB like in the hanging drop method. On the other hand, we observed dispersed several cell clusters in microbeads. The cells in the microbeads proliferated and aggregated into bumpy shapes from several clusters of cells in 2 days. The microbead interior was filled with alginate gel, which hinders direct cell-to-cell interaction. Unlike microbeads, the core of microcapsule was filled with culture medium and the cells aggregated strongly owing to gravity force. More than 80% of core-shell microcapsules generated intact single EB each inside. Hanging drop method is used to aggregate the cells in a droplet by gravity. The cell suspension droplet is injected on the cover of Petri dish by pipetting and it is turned over upside down to attract the cells at the bottom of inverted hemisphere. Injecting more than a hundred hanging drops is a laborious and time-consume work and the ratio of single EB formation is around 70% due to the cell spreading generating satellite small clusters.[36] The microcapsule provided a far better compartment for EC cells than hanging drop method for massive EB formation with comparable uniformity: the average diameter of EBs was 111 μm (C.V. = 12.2%) (Fig. 6(c)). This method is of great advantage in supplying massive and uniform EBs for the study of stem cell differentiation.[37]

 

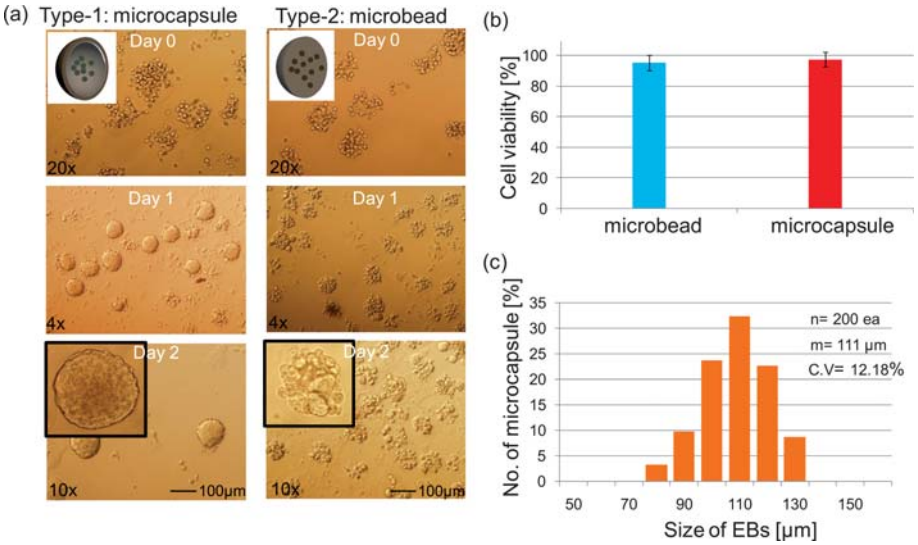


**Fig. 6** The formation of EBs in core-shell microcapsule (type 1) and microbead (type 2). We compared the efficiency of spherical EB formation with P19 EC cells. EC cells were cultured for 2 days in core-shell microcapsules and also in solid microbeads. (a) The cells in microbeads proliferated and aggregated into bumpy shapes from several clusters of cells in two days. Unlike microbeads, the core of microcapsule was filled with culture medium and the cells aggregated strongly owing to gravity force. (b) More than 90% of the cells were alive in both microcapsule and microbeads. (C) More than 80% of core-shell microcapsules generated intact single EB each inside and the average diameter of EBs was 111 μm (C.V. = 12.18%).

## 4. Conclusions

We report the development of a microfluidic chip for generating core-shell microcapsule using 3D coaxial flow. This chip is easier to fabricate and of lower cost than the multi-layered glass capillaries, since the chip needs a simple aligned bonding of two-dimensional structures. Multi-coaxial flow can be readily generated for multi-layered microcapsule by the addition of a focusing channel. The core-shell capsule was applied to effectively form the EBs. It was demonstrated that massive and uniform EB was effectively generated. The hollow microcapsule is potentially applicable to drug delivery, cancer stem cell enrichment or immune-isolation of beta islet cells with high viability. In addition, 3D coaxial flow technology can be exploited in micro flow cytometry, a promising technique for the enumeration of cells and other particles in suspension.

## Acknowledgements

This research was partially supported by the Intelligent Microsystem Center (IMC; http://www.microsystem.re.kr), which is carrying out one of the 21st Century's Frontier R&D Projects sponsored by the Korea Ministry of Commerce, Industry and Energy and also by Pioneer research program for converging technology through the National Research Foundation of Korea funded by the Ministry of Education, Science & Technology. Seok Chung was supported by Seoul R&BD Program (PA090930).

## References

1 G. LindaGriffith and Melody A. Swartz, *Nat. Rev. Mol. Cell Biol.*, 2006, **7**, 211.
2 Cyrille Norotte, Francois S. Marga, Laura E. Niklason and Gabor Forgacs, *Biomaterials*, 2009, **30**, 5910.
3 Ainhoa Murua, Aitziber Portero, Gorka Orive, Rosa Ma Hernández, María de Castro and José Luis Pedraz, *J. Controlled Release*, 2008, **132**, 76.
4 David Wendt, Stefania A. Riboldi, Margherita Cioffi and Ivan Martin, *Adv. Mater.*, 2009, **21**, 3352.
5 Rosanna Gonzalez-McQuire, David W. Green, Kris A. Partridge, Richard O. C. Oreffo, Stephen Mann and Sean A. Davis, *Adv. Mater.*, 2007, **19**, 2236.
6 J. Qian and F. P. Wu, *Chem. Mater.*, 2007, **19**, 5839.
7 A. N. Zelikin, J. F. Quinn and F. Caruso, *Biomacromolecules*, 2006, **7**, 27.
8 Sri Sivakumar, Vipul Bansal, Christina Cortez, Slow-Feng Chong, Alexander N. Zelikin and Frank Caruso, *Adv. Mater.*, 2009, **21**, 1820.
9 O. Kreft, M. Prevot, H. Möhwald and G. B. Sukhorukov, *Angew. Chem., Int. Ed.*, 2007, **46**, 5605.
10 G. B. Sukhorukov, A. L. Rogach, M. Garstka, S. Springer, W. J. Parak, A. Munoz-Javier, O. Kreft, A. G. Skirtach, A. S. Susha, Y. Ramaye, R. Palankar and m. Winterhalter, *Small*, 2007, **3**, 944.
11 W. L. Yuan, G. Hu, L.-Y. W., J. Wu, X. Hu, Z.-G. Su and G.-H. Ma, *Adv. Mater.*, 2008, **20**, 2292.
12 P. F. BNoble, O. J. Cayre, R. G. Alargova, O. D. Velev and V. N. Paunov, *J. Am. Chem. Soc.*, 2004, **126**, 8092.
13 H. Duan, D. Wang, N. S. Sobal, M. Giersig, D. G. Kurth and H. Mohawald, *Nano Lett.*, 2005, **5**, 949.
14 A. A. Antipov and G. B. Sukhorokov, *Adv. Colloid Interface Sci.*, 2004, **111**, 49.
15 Y. Zhang, S. Yang, Y. Guan, W. Cao and J. Xu, *Macromolecules*, 2003, **36**, 4238.
16 K. Bouchemal, S. Briancon, E. Perrier, H. Fessi, I. Bonnet and N. Zydowicz, *Int. J. Pharm.*, 2004, **269**(1), 89.
17 T. Dobashi, T. Furukawa, T. Narita, S. Shimofure, K. Ichikawa and B. Chu, *Langmuir*, 2001, **17**, 4525.
18 E. Lorenceau, A. S. Utada, D. R. Link, G. Cristobal, M. Joanicot and D. A. Weitz, *Langmuir*, 2005, **21**, 9183.
19 E. B. Mock, H. De Bruyn, B. S. Hawkeww, R. G. Gilbert and C. F. Zukoski, *Langmuir*, 2006, **22**, 4037.
20 D. E. Discher and A. Eisenberg, *Science*, 2002, **297**, 967.
21 J. C.-M. Lee, H. Bermudez, B. M. discher, M. A. Sheehan, Y.-Y. Won, F. S. Bates and D. E. Discher, *Biotechnol. Bioeng.*, 2001, **73**, 135.
22 Wei-Heong Tan and Shoji Takeuchi, *Adv. Mater.*, 2007, **19**, 2696.
23 C. Kim, K. S. Lee, Y. E. Kim, K.-J. Lee, S. H. Lee, T. S. Kim and J. K. Kang, *Lab Chip*, 2009, **9**, 1294.
24 S. Sugiura, T. Oda, Y. Aoyagi, R. Matsuo, T. Enomoto, K. Matsumoto, T. Nakamura, M. Satake, A. Ochiai, N. Ohkohchi and M. Nakajima, *Biomed. Microdevices*, 2007, **9**, 91.
25 J. M. Van Raamsdonk and P. L. Chang, *J. Biomed. Mater. Res.*, 2001, **54**, 264.

26 Q. Sun and Y. Deng, *J. Am. Chem. Soc.*, 2005, **127**, 8274.
27 J. Qian and F. Wu, *Chem. Mater.*, 2007, **19**, 5839.
28 L.-Y. Chu, J.-W. Kim, R. K. Shan and D. A. Weitz, *Adv. Funct. Mater.*, 2007, **17**, 3499.
29 C.-H. Choi, J.-H. Jung, D.-W. Kim, Y.-M. Chung and C.-S. Lee, *Lab Chip*, 2008, **8**, 1544.
30 A. S. Utada, E. Lorenceau, D. R. Link, P. D. Kaplan, H. A. Stone and D. A. Weitz, *Science*, 2005, **308**, 537.
31 D. Lee and D. A. Weitz, *Adv. Mater.*, 2008, **20**, 1.
32 Alvaro Mata, Aaron J. Fleischman and Shuvo Roy, *J. Micromech. Microeng.*, 2006, **16**, 276.
33 J. Y. Kim, J. Y. Baek, K. A. Lee and S. H. Lee, *Sens. Actuators, A*, 2005, **119**, 593.
34 R. V. Craster, O. K. Matar and D. T. Papageorgiou, *J. Fluid Mech.*, 2005, **553**, 95.
35 Alexander D. Augst, Hyun Joon Kong and David J. Mooney, *Macromol. Biosci.*, 2006, **6**, 623.
36 H. Kurosawa, T. Imamura, M. Koike, K. Sasaki and Y. Amano, *J. Biosci. Bioeng.*, 2003, **96**, 409.
37 Jaesung Park, Cheul H. Cho, Natesh Parashurama, Yawen Li François Berthiaume, Mehmet Toner, Arno W. Tilles and Martin L. Yarmush, *Lab Chip*, 2007, **7**, 1018.




 